



**HAL**  
open science

## Early effects of different brain radiotherapy modalities on circulating leucocyte subpopulations in rodents

Thao-Nguyen Pham, Julie Coupey, Jérôme Toutain, Serge M Candéias, Gaël Simonin, Marc Rousseau, Omar Touzani, Juliette Thariat, Samuel Valable

► **To cite this version:**

Thao-Nguyen Pham, Julie Coupey, Jérôme Toutain, Serge M Candéias, Gaël Simonin, et al.. Early effects of different brain radiotherapy modalities on circulating leucocyte subpopulations in rodents. *International Journal of Radiation Biology*, 2024, 100 (5), pp.744-755. 10.1080/09553002.2024.2324471 . hal-04504965

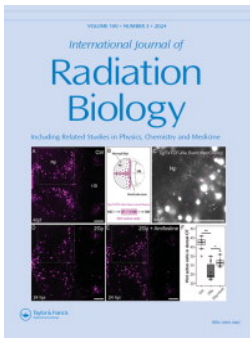
**HAL Id: hal-04504965**

**<https://normandie-univ.hal.science/hal-04504965v1>**

Submitted on 14 Mar 2024

**HAL** is a multi-disciplinary open access archive for the deposit and dissemination of scientific research documents, whether they are published or not. The documents may come from teaching and research institutions in France or abroad, or from public or private research centers.

L'archive ouverte pluridisciplinaire **HAL**, est destinée au dépôt et à la diffusion de documents scientifiques de niveau recherche, publiés ou non, émanant des établissements d'enseignement et de recherche français ou étrangers, des laboratoires publics ou privés.






## Early effects of different brain radiotherapy modalities on circulating leucocyte subpopulations in rodents

Thao-Nguyen Pham, Julie Coupey, Jérôme Toutain, Serge M. Candéias, Gaël Simonin, Marc Rousseau, Omar Touzani, Juliette Thariat & Samuel Valable



To cite this article: Thao-Nguyen Pham, Julie Coupey, Jérôme Toutain, Serge M. Candéias, Gaël Simonin, Marc Rousseau, Omar Touzani, Juliette Thariat & Samuel Valable (11 Mar 2024): Early effects of different brain radiotherapy modalities on circulating leucocyte subpopulations in rodents, International Journal of Radiation Biology, DOI: [10.1080/09553002.2024.2324471](https://doi.org/10.1080/09553002.2024.2324471)

To link to this article: <https://doi.org/10.1080/09553002.2024.2324471>

 View supplementary material 

 Published online: 11 Mar 2024.

 Submit your article to this journal 

 View related articles 

 View Crossmark data 

## Early effects of different brain radiotherapy modalities on circulating leucocyte subpopulations in rodents

Thao-Nguyen Pham<sup>a,b</sup>, Julie Coupey<sup>a</sup>, Jérôme Toutain<sup>a</sup>, Serge M. Candéias<sup>c</sup> , Gaël Simonin<sup>d</sup>, Marc Rousseau<sup>d</sup>, Omar Touzani<sup>a</sup>, Juliette Thariat<sup>b,e†</sup>  and Samuel Valable<sup>a†</sup> 

<sup>a</sup>Normandie Univ, UNICAEN, CNRS, ISTCT, GIP Cyceron, Caen, France; <sup>b</sup>Laboratoire de physique corpusculaire UMR6534 IN2P3/ENSICAEN, France - Normandie Université, France; <sup>c</sup>Univ. Grenoble Alpes, CEA, CNRS, IRIG-LCBM-UMR5249, Grenoble, France; <sup>d</sup>CNRS, IPHC, UMR 7178, Strasbourg University, Strasbourg, France; <sup>e</sup>Department of Radiation Oncology, Centre François Baclesse, Caen, Normandy, France

### ABSTRACT

**Purposes:** Lymphopenia is extensively studied, but not circulating leucocyte subpopulations, which however have distinct roles in tumor tolerance. Proton therapy has been shown to have a lesser impact on the immune system than conventional X-ray radiotherapy through lower dose exposure to healthy tissues. We explored the differential effects of brain X-ray and proton irradiation on circulating leucocyte subpopulations.

**Materials and methods:** Leucocyte subpopulation counts from tumor-free mice were obtained 12 hours after 4 fractions of 2.5 Gy. The relationships between irradiation type (X-rays or protons), irradiated volume (whole-brain/hemi-brain) and dose rate (1 or 2 Gy/min) with circulating leucocyte subpopulations (T-CD4+, T-CD8+, B, and NK-cells, neutrophils, and monocytes) were investigated using linear regression and tree-based modeling approaches. Relationships between dose maps (brain, vessels, lymph nodes (LNs)) and leucocyte subpopulations were analyzed and applied to construct the blood dose model, assessing the hypothesis of a direct lymphocyte-killing effect in radiation-induced lymphopenia.

**Results:** Radiation-induced lymphopenia occurred after X-ray but not proton brain irradiation in lymphoid subpopulations (T-CD4+, T-CD8+, B, and NK-cells). There was an increase in neutrophil counts following protons but not X-rays. Monocytes remained unchanged under both X-rays and protons. Besides irradiation type, irradiated volume and dose rate had a significant impact on NK-cell, neutrophil and monocyte levels but not T-CD4+, T-CD8+, and B-cells. The dose to the blood had a heterogeneous impact on leucocyte subpopulations: neutrophil counts remained stable with increasing dose to the blood, while lymphocyte counts decreased with increasing dose (T-CD8+ cells > T-CD4+ cells > B-cells > NK-cells). Direct cell-killing effect of the dose to the blood mildly contributed to radiation-induced lymphopenia. LN exposure significantly contributed to lymphopenia and partially explained the distinct impact of irradiation type on circulating lymphocytes.

**Conclusions:** Leucocyte subpopulations reacted differently to X-ray or proton brain irradiation. This difference could be partly explained by LN exposure to radiation dose. Further researches and analyses on other biological processes and interactions between leucocyte subpopulations are ongoing. The various mechanisms underlying leucocyte subpopulation changes under different irradiation modalities may have implications for the choice of radiotherapy modalities and their combination with immunotherapy in brain cancer treatment.

### ARTICLE HISTORY

Received 26 September 2023

Revised 13 December 2023

Accepted 9 February 2024





### KEYWORDS

Radiotherapy; proton therapy; immune system; modeling; lymphopenia


## Introduction

Radiotherapy is a cornerstone of cancer treatment and is used in 60% of patients with solid tumors (Orth et al. 2014), including brain tumors. In recent years, there has been renewed interest not only in immunotherapy but also in developing synergistic radiotherapy and immunotherapy combinations (Wu et al. 2017). This means accounting for the stimulatory or suppressive immune effects of radiotherapy and its effects on immune cells at the tumor and tissue levels, including blood.

For example, acute radiation-induced lymphopenia (RIL) (Ellsworth 2018; Holub et al. 2020) has been associated with reduced tumor response to immune checkpoint inhibitors (Ménétrier-Caux et al. 2019) and with an increased risk of recurrence and poorer survival. RIL may occur due to irradiation of the circulating blood pool of lymphocytes. In addition to lymphocytes, myeloid cells can either promote or control tumor growth, depending on their subtypes. Neutrophils, the most abundant myeloid cells, have also emerged as regulators of cancer. High circulating neutrophil-to-lymphocyte ratios

**CONTACT** Samuel Valable  [samuel.valable@cnrs.fr](mailto:samuel.valable@cnrs.fr)  Normandie Univ, UNICAEN, CNRS, ISTCT, GIP Cyceron, Caen, France; Juliette Thariat, MD, PhD  [jthariat@gmail.com](mailto:jthariat@gmail.com)  Laboratoire de physique corpusculaire UMR6534 IN2P3/ENSICAEN, France - Normandie Université, France.

†These authors contributed equally to this work.

 Supplemental data for this article can be accessed online at <https://doi.org/10.1080/09553002.2024.2324471>.

© 2024 CNRS.

have been shown to be a robust prognostic factor of poor clinical outcome in various cancers undergoing different modalities of cancer treatment, including radiotherapy, chemotherapy, and immunotherapy (Cho et al. 2018).

Radiotherapy technologies have improved toward more precise dose delivery (Thariat et al. 2013; de Andrade Carvalho and Villar 2018). For instance, the use of protons instead of conventional radiotherapy using X-rays can achieve better normal tissue sparing using a smaller entrance dose, no exit dose, and small lateral beam penumbra, which could translate into a better therapeutic ratio (Murshed 2019). Proton therapy is performed for various brain tumors (Lesueur et al. 2019) and has shown less severe RIL compared to X-rays (Mohan et al. 2021). By lowering the immunosuppressive effect, the use of proton beam might provide a better synergy with immunotherapy (Gaikwad et al. 2023). However, the different effects of protons on myeloid cells and lymphocyte subpopulations have not yet been sufficiently studied. In addition to irradiation type (X-rays or protons), other radiotherapy parameters, such as dose to the blood, fractionation, tumor and tissue volumes and timing, have a direct impact on leucocyte subpopulations (Yovino et al. 2013; Ellsworth et al. 2022). Beyond lymphocytes, the mechanisms underlying the effects of radiation on circulating leucocytes, including lymphoid and myeloid cells, are incompletely understood (Pham et al. 2023).

Previous studies proposed that RIL is a result of the direct exposure of circulating lymphocytes to radiation during the irradiation period, i.e., direct cell-killing effect (Yovino et al. 2013; Ladbury et al. 2019; Hammi et al. 2020; Chen et al. 2022). This hypothesis is supported by the observed high radiosensitivity of lymphocytes *in vitro*, where a dose of 2Gy leads to only 10% lymphocyte survival (Nakamura et al. 1990). Protons have been shown to induce higher rates of radiation-induced cell death in lymphocytes compared to X-rays *in vitro* (Miszczyk et al. 2018), suggesting that the lymphocyte-sparing effects of protons are due to more spatially targeted irradiation.

This study aims at investigating the effects of different modalities of conventional radiotherapy (X-rays) and proton irradiation on circulating leucocyte subpopulations in rodent using statistical models. We designed an experimental protocol using a murine model to investigate and understand the mechanisms of the differences between conventional radiotherapy (X-rays) and proton irradiation on leucocyte subpopulations. We incorporated physiological data knowledge to further understand the effects (direct/indirect) of radiation beams on circulating leucocyte subpopulations. Statistical regression models were applied to investigate the relationships between radiation parameters and physiology-based parameters and their impact on leucocyte subpopulations.

## Materials and methods

### Data

Animal experiments allow studies of many more parameters than human studies with replicability using subjects with

identical characteristics. Tumor-free animal models can provide important mechanistic insights into the interactions between radiotherapy and leucocytes independent of the interaction between leucocytes and the tumor microenvironment. Two preclinical experiments investigated the effects of X-ray or proton brain irradiation on leucocyte populations in 96 healthy, tumor-free C57BL/6 adult mice. Animal experiments were performed in accordance with the current European regulations, with permission of the regional committee on animal ethics CENOMEXA for the experiments carried out in Caen (#27343, for X-ray experiments) and CEEA035 for those performed in Strasbourg (#27413, for proton experiments). In each experiment, 40 mice received 10Gy in 4 twice-daily fractions (2.5Gy) for 2 consecutive days of either X-ray or proton, and blood samples were collected 12 hours after the last fraction. The choice of this time point aimed to study the acute effect of brain irradiation on leucocyte subpopulations before the initiation of their recovery (Coupey et al., 2024). Flow cytometry was used to quantify the frequency of leucocyte subpopulations in the blood, including T-CD4<sup>+</sup>-cells, T-CD8<sup>+</sup>-cells, B-cells, and NK-cells from the lymphoid population; neutrophils and monocytes from the myeloid population. Radiation parameters included irradiation type (photon(X-ray)/proton), irradiated volume (whole-brain or hemi-brain) and dose rate (1 or 2Gy/min). Eight non-irradiated mice were used as controls in each experiment (Figure 1A).

The full detailed experimental protocol for mouse irradiation, blood collection, flow cytometry and gating strategy are presented in supplementary and in Coupey et al. 2024, submitted. Each cell population concentration was normalized to the ratio over the control group in each experiment, with the reference baseline concentration fixed at value 1.

### Impact of radiation parameters on leucocyte subpopulation levels

Analyses were performed separately for all six leucocyte subpopulations. Linear regression using univariable analysis (UA) was first applied for the three radiation parameters (irradiation type/irradiated volume/dose rate). Backward stepwise multivariable analysis (MA) was then performed to determine the most significant predictor(s) for each leucocyte subpopulation among variables obtained from UA and investigate the additive interaction between the predictors. Multiplicative interaction analysis (IA) was also performed. Multiple MA was applied to assess correlations between parameters and leucocyte subpopulations following linear regression analysis. The model selection was based on the Akaike information criterion. All analyses were performed using R studio version 4.1.2 (R Core Team 2021).

A tree-based approach was also used to analyze the existence of any hierarchical interactions between radiation parameters and leucocyte subpopulations. The tree was built using the mean squared error (MSE) for splitting node decisions; specifically, the node splitting strategy minimized the MSE. The splitting process stopped

when there was no further possible split. This procedure was performed using the *rpart* package version 4.1.19 (Therneau et al. 2022). A post-pruning process was performed to remove nonsignificant branches. The MSE was calculated as

$$\text{MSE} = \frac{(\text{Prediction}_i - \text{Observation}_i)^2}{N} \quad i = 1, N$$

Parameter importance ranking was obtained by random forest regression in terms of MSE increment (%IncMSE) when imputing the parameters from the model. A stronger impact of radiation parameters is reflected by a higher %IncMSE.

### Effect of direct radiation exposure on circulating leucocyte subpopulations

The animal radiotherapy software (treatment planning system SmarT-PLAN, Precision X-ray, was applied to provide a brain irradiation dose map for each animal in the X-ray group. The proton treatment plan based on a CT scan was carried out using Monte Carlo simulation software GATE (Geant4 Application for Tomographic Emission) version 9.1.

The total dose delivered to the mice was four fractions of 2.5 Gy delivered to either the whole or hemi-brain. We estimated the dose to the blood, using total blood flow and  $V_{\text{blood}}$  with 3 assumptions (0). First, the dose distribution was assumed to be distributed directly and uniformly from the radiation beam during irradiation without interaction with surrounding tissues. Second, each unit of  $V_{\text{blood}}$  spent the same amount of time crossing the radiation beam. There is no organ distribution or clearance of blood during irradiation. Blood pressure fluctuations on  $V_{\text{blood}}$  and blood flow in the irradiated area were neglected (during our experiments, mice were under anesthesia with a fixed breathing rate of 40 breaths/min to reduce inter-animal heterogeneity). Third, when entering the irradiated area, a unit of  $V_{\text{blood}}$  received a certain radiation dose equal to the product of the dose rate and mean transit time (MTT) in the irradiated area. After leaving the irradiated area, the irradiated volume will be diluted within the whole  $V_{\text{blood}}$  immediately. From those assumptions, it is possible to estimate the certain amount of blood receiving a dose higher than 0, 0.1, 0.2, 0.3, or 0.4 Gy.

The model was separated into two compartments (Figure 1C), including the blood in the irradiated area and blood in nonirradiated area, represented by their volumes and the MTT that a blood particle spends in the irradiated area; where the dose rate is denoted as RR (Gy/s) and the MTT

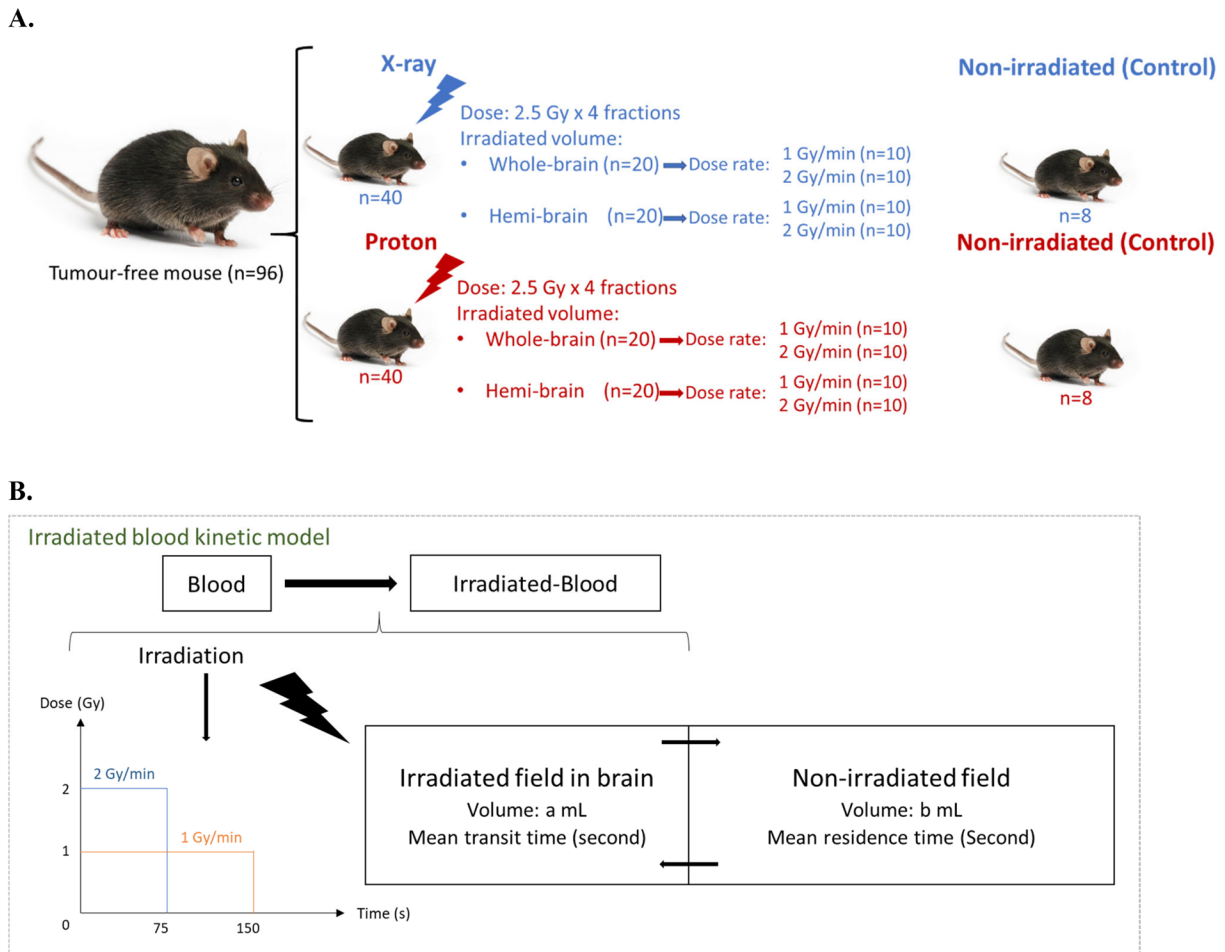


Figure 1. General structural model of radiation dose distribution in blood.

is denoted as MTT (s). Each time passing through the irradiated area, each blood particle will receive  $RR \cdot MTT$  (Gy). Let  $V_{t(s)}^{Irr}$  and  $V_{t(s)}^{Non-irr}$  be the vectors for the dose distribution in the irradiated area and non-irradiated area, respectively, at time  $t$  (s):

$$\begin{cases} V_t^{Irr} = (V_{t,0Gy}^{Irr}, V_{t,xGy}^{Irr}, V_{t,2xGy}^{Irr}, \dots, V_{t,nxGy}^{Irr}) \\ V_t^{Non-irr} = (V_{t,0Gy}^{Non-irr}, V_{t,xGy}^{Non-irr}, V_{t,2xGy}^{Non-irr}, \dots, V_{t,nxGy}^{Non-irr}) \end{cases}$$

At  $t = t_0 + MTT$ , the blood in the irradiated area receives  $x$  Gy and leaves the irradiated area, replaced by another volume from the non-irradiated area.

$$\begin{cases} V_{t,kxGy}^{Irr} = V_{t-MTT,kxGy}^{Non-irr} \\ V_{t,kxGy}^{Non-irr} = p \cdot V_{t-MTT,(k-1)xGy}^{Irr} + (1-p) \cdot V_{t-MTT,kxGy}^{Non-irr} \end{cases}$$

$$\text{where } p = \frac{\text{Volume}_{\text{Irradiated area}}}{\text{Volume}_{\text{Non-irradiated area}} - \text{Volume}_{\text{Irradiated area}}}$$

At  $t = 0$  (before irradiation), 100% of blood receives 0 Gy, so  $V_{t=0s} = (1, 0, 0, \dots, 0)$ . After finishing the simulation, the overall radiation dose distribution in blood is calculated as

$$V = q \cdot V^{Irr} + (1-q) \cdot V^{Non-irr}$$

$$\text{where } q = \frac{\text{Volume}_{\text{Irradiated area}}}{\text{Volume}_{\text{Non-irradiated area}} + \text{Volume}_{\text{Irradiated area}}}$$

The blood flow volume in the irradiated area is approximately 0.26 mL/min (Hall et al. 2012) for both X-ray and proton irradiation. For hemi-brain irradiation, the blood flow volume in the irradiated area was 0.13 mL/min. The mean transit dose to the blood (MTD) is the dose that

blood receives when passing through the irradiated area. MTD is calculated as the product of the mean time of residence of the blood in the irradiated area (MTT) and dose rate.

Beyond the blood, lymph nodes (LNs) also contain large amounts of lymphocytes and are where priming occurs to transform naïve lymphocytes into mature effector lymphocytes (Pham et al. 2023). Nodal irradiation can interfere with lymphocyte survival and priming. The number of LNs in irradiated area was determined. Impact of the dose to the blood and number of LNs in the irradiated area on leucocyte subpopulations was analyzed using linear regression analysis and parameter selection with the same method as mentioned in section 2.2.

## Results

X-rays caused a significant reduction of 50% of circulating lymphocytes (T-CD4<sup>+</sup>, T-CD8<sup>+</sup>, B and NK-cells) as early as 12 hours after the last fraction of irradiation. This early effect could be recovered since day 3 after the last irradiated fractions till day 24. The change in lymphoid subpopulations was not observed following proton irradiation. A significant increase in neutrophils and almost no change in monocytes were noticed after proton irradiation (Figure 2).

### Impact of radiation parameters on leucocyte subpopulation counts

We analyzed the impact of radiation parameters (irradiation type, irradiated volume and dose rate) on the 6 leucocyte subpopulations (T-CD4<sup>+</sup>, T-CD8<sup>+</sup>, B, NK, neutrophils and monocytes) using linear regression and tree-based modeling. On univariable analysis, irradiation type and irradiated volume had a significant impact on lymphoid but not myeloid subpopulations. Dose rate alone did not have any significant impact on all leucocyte subpopulations. Multiple multivariable analysis provided the correlation between

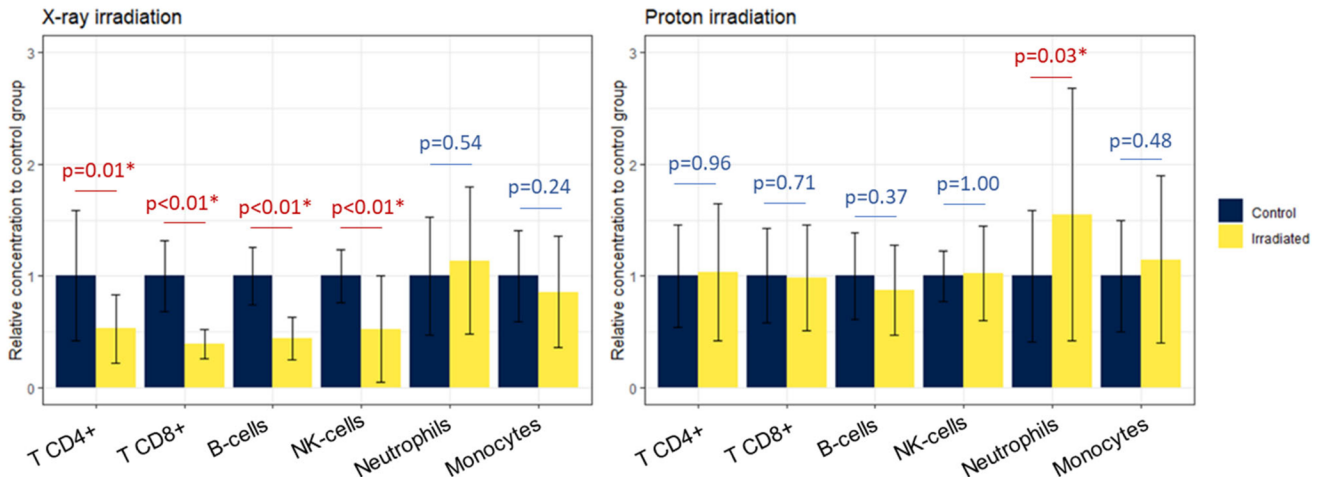
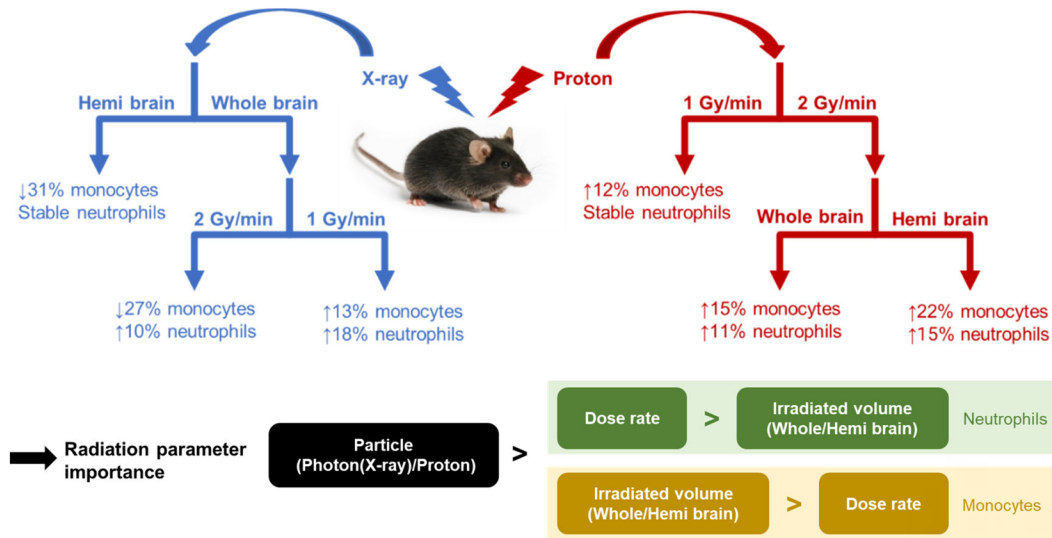


**Figure 2.** Leucocyte subpopulation counts in mice undergoing X-ray or proton irradiation. Leucocyte subpopulations include T-CD4<sup>+</sup> cells, T-CD8<sup>+</sup> cells, B-cells, NK-cells, neutrophils, and monocytes. Error bars represent the standard deviation ( $n=8$  for control and  $n=40$  for irradiated groups). The Mann-Whitney  $U$  test was used to test if there was a difference between the irradiated and non-irradiated groups.

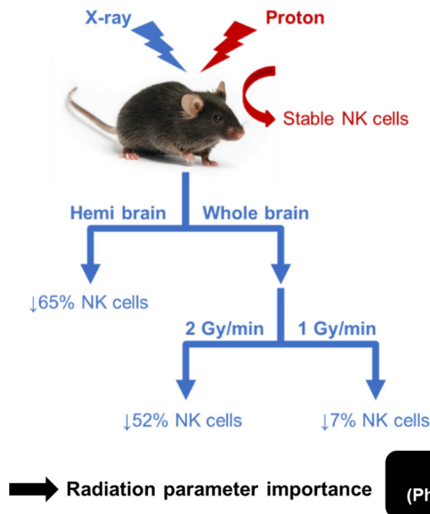


A.



B.

B.1.



B.2.

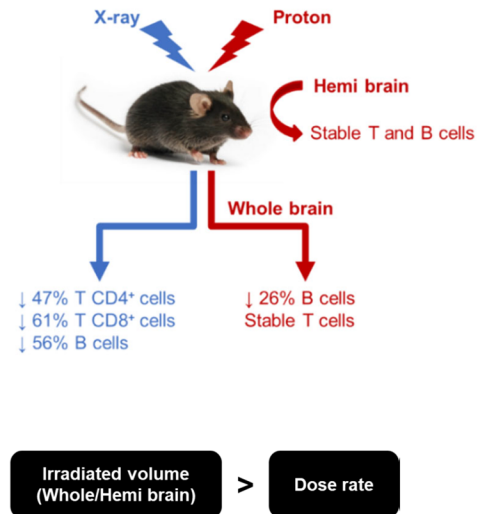


**Figure 3.** Tree-based analysis of radiation parameter importance of leucocyte subpopulations changes. Parameter importance was determined based on random forest regression analysis for the six leucocyte subpopulations, including (A) Myeloid subpopulations, (B) Lymphoid subpopulations, of which (B.1) NK-cells, and (B.2) T-CD4<sup>+</sup> cells, T-CD8<sup>+</sup> cells, and B-cells.

parameter estimation of leucocyte subpopulations following linear regression analysis (see [supplementary Figure 4](#) for details). The correlation was weak between radiation parameters but high among the various leucocyte subpopulations. Specifically, between leucocyte subpopulations, there was a high correlation between either irradiation type, irradiated volume, or dose rate within the myeloid lineage (neutrophils and monocytes) and between T-CD4<sup>+</sup>, T-CD8<sup>+</sup>, and B cells. The impact on NK cells were independent of the effects on other leucocyte subpopulations. This correlation suggests that there is an interaction between leucocyte subpopulations under brain irradiation. Using parameter stepwise backward selection, only irradiation type had a significant impact on lymphoid subpopulations. Linear regression with interaction analysis showed a significant interaction of radiation parameters on B-cells, NK-cells and myeloid subpopulations. Interaction analysis showed a

complex interplay between irradiation type, irradiated volume and dose rate for NK-cells and myeloid subpopulations. This interplay could be further investigated using a tree-based model.

A tree-based model provided an easy-to-visualize model ([Figure 3](#)): The non-linear interaction between predictors appeared more pronounced for myeloid than lymphoid populations. The tree-based models of myeloid subpopulations were more complex than those of lymphoid subpopulations. This is corresponding to the result of interaction analysis in the linear regression model. The splitting procedures were different between X-rays and protons arms in the myeloid cell model. With X-rays, the irradiated volume was more important than the dose rate, while the dose rate was more important than the irradiated volume with protons ([Figure 3A](#)). This implied a difference in acute radiation-induced myeloid cell variation between the two irradiation types.

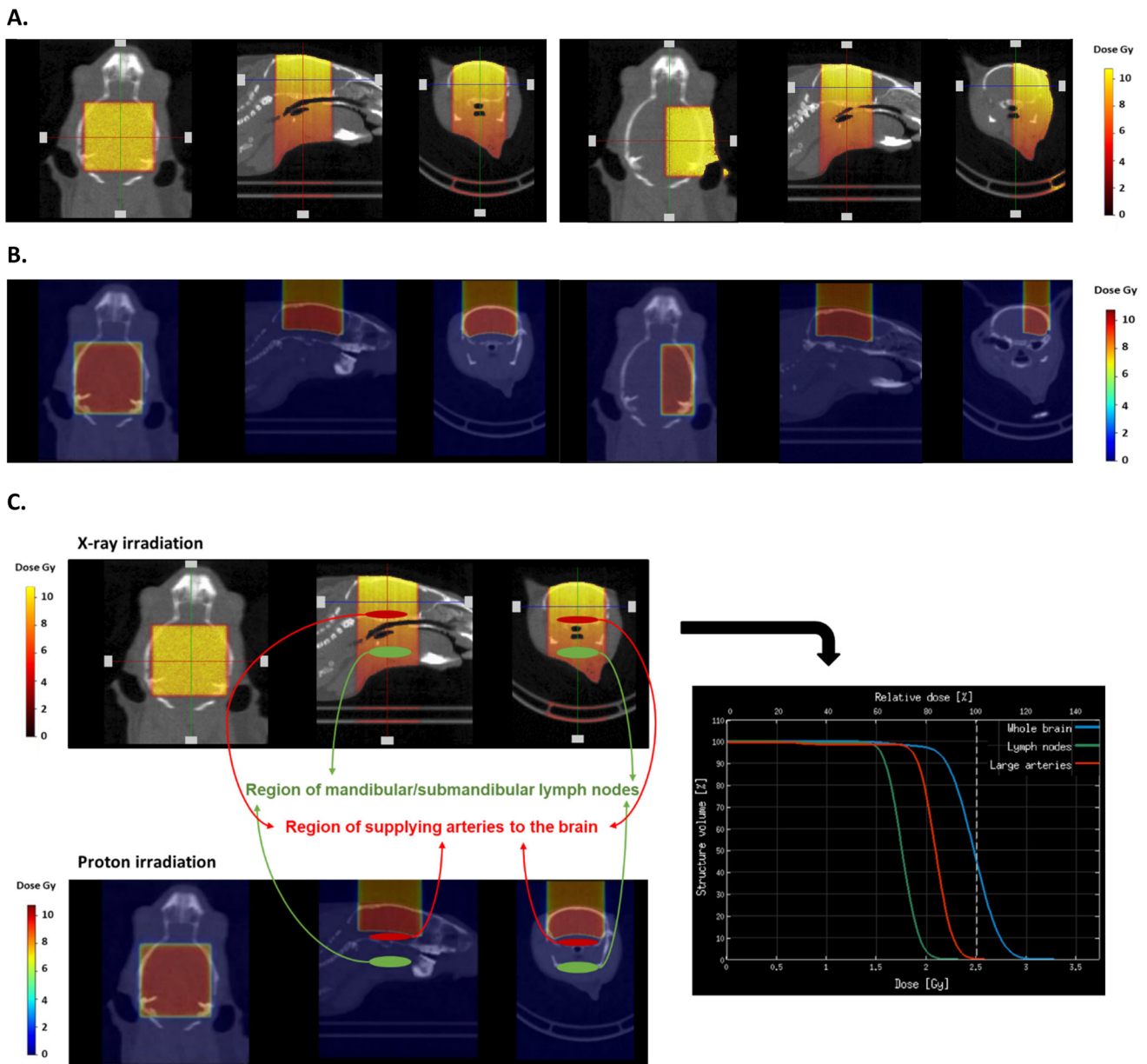


**Figure 4.** Dose distribution using Monte-Carlo simulation software of whole-brain irradiation using either an X-ray beam (A) or a proton beam (B). (C) Distinct effect of blood and lymph nodes exposure to radiation dose between X-rays and protons.

Among lymphocytes, the NK-cell's tree-based model indicated that severe acute reduction occurred following irradiation when using X-rays on a small volume (hemi-brain) (Figure 3B.1). For the larger volume (whole-brain), an important NK-cell reduction was observed only when dose rate was high (2Gy/min). For T and B-cells, lymphopenia could be simply explained by differences in irradiation type: X-rays induced lymphopenia, which did not occur with protons (for T-cells) or occurred only in a larger irradiated volume (for B-cells) with a lower severity than with X-rays (Figure 3B.2).

From random forest analysis, parameter importance ranking returned irradiation type as the most important predictor, followed by irradiated volume and dose rate in all leucocyte subpopulations except for neutrophils (for which dose rate was more important than irradiated volume)

(Figure 3). Irradiation type had a stronger impact on lymphocytes (strongest on T-CD8<sup>+</sup> cells, followed by NK-cells, B-cells and T CD4<sup>+</sup> cells) than on myeloid cells.

#### **Explanation of the stronger effects of X-ray versus proton brain irradiation on circulating leucocytes through direct radiation exposure**

Brain irradiation dose maps of X-rays or protons are presented in Figure 4. Supplying cerebral arteries (anterior cerebral arteries, middle cerebral arteries, internal carotid arteries, posterior cerebral arteries, superior cerebellar arteries, and basilar arteries) contain circulating lymphoid/myeloid cells. They were within the irradiated area using X-ray beams while proton beams spared internal carotid



**Table 1.** Estimated supplying brain artery volume in the irradiated area and physiology-based parameters for radiation subgroups.

Supplying artery volume in irradiated area								
Particle	X-ray				Proton			
	Volume (mL)							
Total cerebral blood	0.0200				0.0200			
Internal carotid arteries	0.0002				0			
Basilar artery	0.0002				0			
Total	0.0204				0.0200			
Physiology-based parameters for radiation subgroups								
Particle	X-ray				Proton			
	Whole-brain		Hemi brain		Whole-brain		Hemi brain	
Irradiated volume	1	2	1	2	1	2	1	2
Dose rate (Gy/min)	1	2	1	2	1	2	1	2
Total blood volume in irradiated area (mL)	0.0204	0.0204	0.0102	0.0102	0.0200	0.0200	0.0100	0.0100
Blood flow volume in irradiated area (mL/min)	0.26	0.26	0.13	0.13	0.26	0.26	0.13	0.13
Mean transit time in irradiated area (s)	4.71	4.71	4.71	4.71	4.62	4.62	4.62	4.62
Mean transit dose (Gy)	0.08	0.16	0.08	0.16	0.07	0.15	0.07	0.15
Number of lymph nodes irradiated	4	4	2	2	0	0	0	0

arteries, posterior cerebral arteries, superior cerebellar arteries, and basilar arteries (Figure 4C; volume of arteries in C57BL/6 mice (Ghanavati 2017) in Table 1).

These arteries supplied blood to the whole-brain, so the amount of blood passing through those arteries per time unit (total blood flow) was approximately equal to the total cerebral blood flow. Details of blood volume, blood flow, MTT and number of LNs in the irradiated area are described in Table 1. The total volume of blood in the supplying arteries was small compared to the total cerebral blood volume. Thus, total blood volume and blood flow in the irradiated area was not considerably different between X-Rays and protons. On the other hand, there was a smaller blood volume irradiated in hemi-brain compared to whole-brain irradiation, which however resulted in similar T-CD4<sup>+</sup>, TCD8<sup>+</sup> and B lymphopenia in the X-ray experiment. NK lymphopenia was even greater in hemi-brain compared to whole-brain irradiation. This implied that blood exposure to radiation dose had a modest role in causing RIL. Paired or single mandibular and accessory mandibular LNs were exposed to X-rays but not protons after whole or hemi-brain X-ray irradiation, respectively (Figure 4C). Thus, in X-ray irradiation, the number of irradiated LNs is 4 in whole-brain irradiation and 2 in hemi-brain irradiation. Those LNs were not irradiated when proton irradiation was delivered.

The delivery of 4 fractions of 2.5Gy to the brain (X-rays/protons) resulted in almost no blood volume receiving higher than 0.8Gy (Figure 5A). We further extracted the volume of blood receiving a dose higher than a discretized dose threshold (V<sub>0</sub>, V<sub>0.1</sub>, V<sub>0.2</sub>, V<sub>0.3</sub>, V<sub>0.4</sub>) to analyze the impact of small radiation dose exposure on circulating leucocyte subpopulation count.

Univariate analysis showed that all five discretized dose parameters were predictors of variations in the lymphoid subpopulations. None of these parameters were significant for the myeloid subpopulations. Figure 5B shows the variation in the percentage of the leucocyte subpopulation with each additional 1% of V<sub>blood</sub> above a given dose threshold. Twelve hours after delivery of the last fraction, neutrophil levels were stable when exposing the blood to increasing doses. Lymphocyte levels decreased with increasing dose

(T-CD8<sup>+</sup>-cells > T-CD4<sup>+</sup>-cells > B-cells > NK-cells), especially above 0.3Gy (see supplementary Table 2 for details).

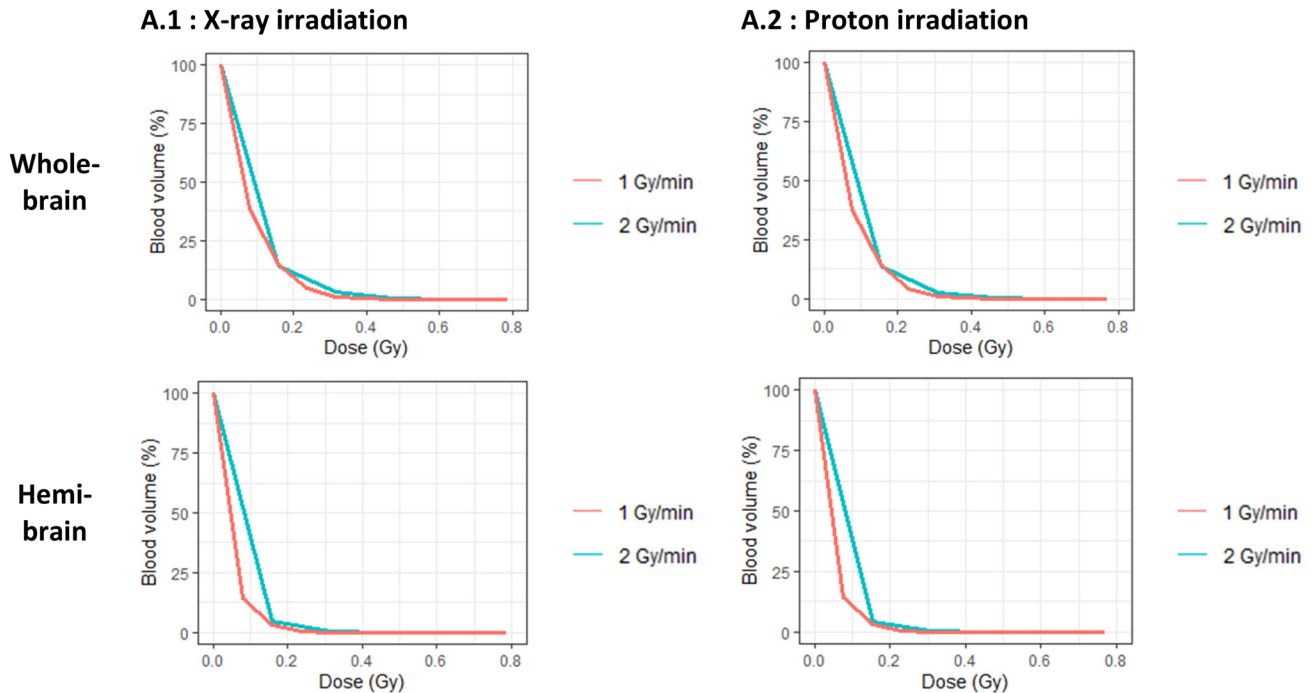
V<sub>blood</sub> receiving no dose (V<sub>0</sub>) was chosen for regression analyses together with the number of LNs irradiated and MTD delivered to the blood. On UA, all physiology-based parameters (including irradiated blood volume and LNs exposure to radiation) were predictors of lymphocyte subpopulation levels. On backward stepwise MA, significant predictors only included the number of irradiated LNs. Thus, the differential effect of brain irradiation on leucocytes could be explained by the different exposure of LNs and blood to radiation, with LN exposure the predominant factor (see supplementary Table 3 for details).

## Discussion

Radiotherapy has been identified as a potential partner for immunotherapy owing to its immunostimulatory effects (Galluzzi et al. 2023). On the other hand, radiotherapy also promotes immunosuppression, noticeably through its effect on circulating leucocytes (Zhang et al. 2022), which highly impacts the effectiveness of immunotherapy. Understanding the factors underlying radiation-induced variations in circulating leucocytes is essential to optimize radiotherapy-immunotherapy combinations. As a first approach, we used tumor-free animal models to provide mechanistic insights into the interactions between ionizing radiation delivery and leucocytes independently on the interaction between leucocyte and the tumor microenvironment.

In addition to irradiation type, irradiated volume (including the number of LNs) and dose rate have a direct impact on leucocyte subpopulation counts in the blood. Pioneer clinical studies showed a correlation between irradiated volume and lymphocyte nadir in brain, lung, and esophageal cancers (Tang et al. 2014; Huang et al. 2015), which is also in line with the importance of the irradiated volume on lymphopenia detected in our results. The type of irradiation impacts the size of the irradiated area. Using vertical X-ray irradiation of the mouse brain, the chin and neck (which contain large arteries supplying the brain) were also included in the irradiated area. These structures are not irradiated with proton beam ballistics due to the absence of an exit dose after the Bragg peak. The

A.



B.

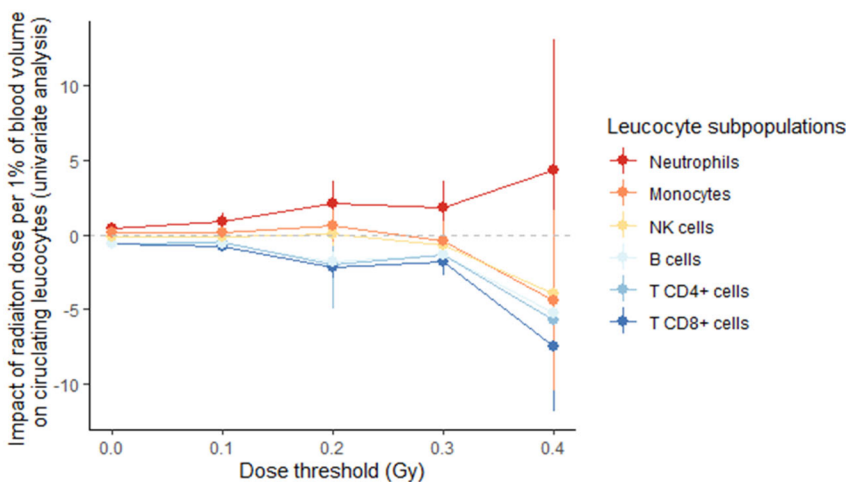


**Figure 5.** (A) Dose volume histogram of blood after delivery of four fractions of 2.5 Gy to the brain. The blood dose simulation was based on a cerebral blood volume of 0.02 mL and cerebral blood flow volume of 0.26 mL/min (Hall et al. 2012). Simulation details are provided in 0. The y-axis represents the percentage of blood volume, and the x-axis represents the dose. The figures show the percentage of blood volume receiving at least a given dose. (B) Blood dose parameters in relationship with leucocyte.

difference between blood vessel volumes in the irradiated area led to a higher fraction of irradiated blood with X-rays compared to protons. Similarly, X-ray beams irradiate the chin/neck LNs, structures rich in lymphocytes. LNs are critical for activation of naïve lymphocytes, before activated lymphocytes recirculate and exert their immune functions. In fact, only a small number of lymphocytes are circulating lymphocytes (Blum and Pabst 2007), and most peripheral blood lymphocytes were only exposed to a very small radiation dose (Figure 5A). These data are in line with our results, showing that blood irradiation could not solely explain the lymphocyte drop of nearly 50% that we observed.

Most of the previous blood dose simulations showed that increasing the dose rate would reduce the amount of blood, and circulating lymphocytes, exposed to radiation (Yovino et al. 2013; Hammi et al. 2020). Here, the dose rate alone did not show a significant effect on leucocyte subpopulations. However, there were significant interactions with other radiation parameters for innate immune cell subpopulations (NK cells, neutrophils, and monocytes). The dose rate was positively correlated with the MTD and negatively correlated with radiation exposure time. Radiation parameter manipulation might reveal some potential for high-dose rate irradiation, or ultra-fast radiation treatment (FLASH) to spare circulating lymphocytes and reduce the likelihood of

radiation-induced lymphopenia (Jin et al. 2020). Due to the modest direct effect of dose rate on RIL, increasing dose rate to investigate whether it results in lower lymphopenia rates might not be sufficient. A recent study on cardiac and splenic irradiation in rodents showed that an ultra-high dose rate (35 Gy/s) did not protect lymphocyte subpopulations from the effects of X-ray irradiation (Venkatesulu et al. 2019). Herein, the dose rate only ranged from 1 to 2 Gy/min, and further studies using high or ultra-high dose rates are warranted.

Similarly to lymphopenia, an expansion in myeloid subpopulations before and following cancer treatment is considered to have a negative impact on overall survival and treatment benefits of either radiotherapy, chemotherapy, or immunotherapy (Cho et al. 2018; Bilen et al. 2019). Unlike lymphocytes, myeloid cells are radioresistant (Pham et al. 2023). The impact of brain radiotherapy on myeloid cells has been less studied than on lymphocytes. In theory, radiation should exert a cell-killing effect on all cell lineages. However, a strong impact of cell killing through direct exposure to radiation is unlikely to be visible on myeloid cells due to their short half-life and high renewal rate (Pham et al. 2023). It was reported that granulocyte function *in vitro* was unaffected by doses of up to 400 Gy (Holley et al. 1974), and most studies investigating the impact of radiation on monocytes *in vitro* delivered > 25 Gy (Buescher and Gallin 1984). Thus, four fractionated doses of 2.5 Gy were unlikely to cause any large direct killing effect for neutrophils and monocytes, as observed in our study. It was previously reported that macrophages present in the tumor bulk are resistant to X-rays (Leblond et al. 2017). Radiation-induced neutropenia or monocytopenia was mostly reported in cases where bone marrow was highly exposed to radiation (Farese et al. 2015; Macintyre et al. 2021). In brain irradiation, a very small amount of bone marrow in the skull is exposed to radiation; thus, neutropenia or monocytopenia is unlikely to appear. In contrast, in our analysis, proton brain irradiation caused a significant increase in neutrophil counts. The sudden and early increase in neutrophil numbers following irradiation has already been observed in rhesus macaques after a single dose (6 Gy) of total body X-ray irradiation before the neutropenia caused by bone marrow dysfunction became apparent (Farese et al. 2015; Macintyre et al. 2021). An increase in neutrophil count could be caused either by stimulated granulopoiesis as a feedback function for acute neutropenia, which is unlikely to occur here as explained above (Holley et al. 1974), or in response to injury (Widick and Winer 2016). Since the data we used were from fractionated irradiation, the observed increase in neutrophil counts most likely results from the rebound in granulopoiesis that takes place after each fraction.

The high rate of cell depletion in all lymphoid populations after X-rays but not protons *n vivo* in our results is in line with simulation data (Hammi et al. 2020) and with clinical data reporting that the use of proton beams in radiotherapy could reduce the likelihood of lymphopenia compared to photon beams (Mohan et al. 2021). In fact, lymphocytes are among the most radiosensitive cells in mammals (Pham et al. 2023). Lymphocyte depletion following radiation exposure could be due to either a direct cell-killing effect or cell-killing

mediated by local/systemic inflammation or interactions between irradiated tissues, including the tumors and the immune system. The difference between each subpopulation's response to brain irradiation could be linked to intrinsic cellular radiosensitivity or to interactions between cell subtypes. Using preclinical data, we derived knowledge on tumor-free individuals, thus ignoring the interactions of tumors and the immune system. This allowed us to further understand the mechanisms behind radiation-induced variations in circulating leucocyte counts.

Initially, our modeling setup assumed a similar biological effect of X-rays and protons, using the common correction factor of 1.1 for relative biological effectiveness (Murshed 2019). Differences in early cell-killing following *n vitro* irradiation of lymphocytes with X-rays or protons have, however, been reported: 4 hours after irradiation, protons caused a higher rate of necrotic cell death than X-rays (Miszczyk et al. 2018). The radiosensitivity of lymphocytes as they pass through the treated area has long been known (Shohan 1916) and prior studies have shown that RIL is correlated to the dose delivered to the circulating blood (Yovino et al. 2013). Our UA of blood dose parameters suggest that the dose received by a given volume is likely to be a significant predictor of reduced lymphocyte subpopulation counts. However, analysis of the dose to the blood data revealed that lymphocyte loss following irradiation *in vivo* is higher than lymphocyte loss from direct exposure to radiation. In fact, the amount of blood exposed to radiation during brain irradiation is small (approximately 1% of the total blood volume) and insignificantly different between X-ray and proton experiments. Also, within our X-ray experiments, lymphopenia occurred similarly between whole-brain and hemi-brain irradiation, where there is a considerable difference in blood volume exposed to radiation dose. The four LNs in the irradiated area were also small LNs. These observations suggest that direct lymphocyte exposure to radiation in the blood was not enough to explain the high reduction in lymphocytes following brain X-ray irradiation.

For lymphocytes, the contribution of the direct cell-killing effect to overall lymphopenia is also modest. Following a sudden drop, blood lymphocyte counts nearly reached their initial levels in less than 3 hours by lymphocyte recruitment from lymphatic organs, according to simulation from recirculation models (Pham et al. 2023). Thus, a reduction in lymphocytes 6 hours after the last irradiation fraction could be due to the depletion of both circulating and homing lymphocytes. This is the result of a combination of direct radiation-induced death and the depletion of lymphocyte reserves in secondary organ stores after four consecutive exposures. Indeed, our results demonstrated that the presence of LNs in the irradiated area is an important predictor of circulating lymphocyte depletion.

On the other hand, radiotherapy can deplete circulating lymphocytes indirectly through its effects on innate and adaptive immunity by various mechanisms: radiotherapy elicits tumor cell death and subsequent release of tumor antigens, which induce the immune response; radiotherapy is a potent inducer of cytokines, which alter the profile and function of immune infiltrates; and radiotherapy can

remodel the stromal and vascular compartments of the tumor microenvironment (Ahmed et al. 2013). The induction of cytokines is a potential explanation for RIL in a tumor-free model. The effects of irradiated plasma on non-irradiated lymphocytes have been investigated since 1968 (Hollowell and Littlefield 1968). The frequency of chromosome and chromatid breaks increased when lymphocytes were co-cultured with irradiated plasma of radiotherapy-treated cancerous patients compared to non-irradiated plasma from either cancerous or healthy patients (Hollowell and Littlefield 1968). Thus, the mechanisms of RIL include mechanisms other than direct cell exposure to radiation. A modest contribution of direct cell exposure to RIL was observed in blood irradiation *ex vivo* in rodents, in which severe lymphopenia occurred even when only 10% of blood was directly exposed to a radiation beam outside the body and then reinjected into the mice. (Kapoor et al. 2015).

Unlike T/B-cells, NK-cells were reported to be a radio-resistant population both *in vitro* and *in vivo*, even after whole-body irradiation (Park and Jung 2021). Therefore, the reduction in NK-cells following fractionated brain irradiation in these experiments was less likely to result from the same mechanisms as other lymphocyte populations. Brain injury/neuroinflammation could be an explanation for the depletion of NK-cells following X-ray irradiation. NK-cell reduction at the systemic level was reported in glioblastoma patients following chemoradiotherapy treatment (Fadul et al. 2011) due to the secretion of mediators that induced NK-cell infiltration. At the tissue level during neuroinflammation, NK-cell infiltration was reported to attract and control neutrophil and monocyte infiltration of the brain by chemokine secretion (He et al. 2016). In fact, our results demonstrated that the impact of radiation on NK-cells was more complicated than that on T/B-cells as observed in the interaction linear regression and tree-based analysis.

## Conclusions

The modeling of our results in the context of physiology-based parameters provided new insights into the effects of radiation on the immune system. Brain irradiation with X-rays or protons exerts different effects on circulating leucocyte levels. The irradiated volume and dose rate impact myeloid cells differently between X-rays and protons. The conservative effect of proton brain irradiation compared to X-rays explained by the direct cell-killing effect of the radiation dose to the blood is modest. The existence of LNs in the irradiated area significantly explained the different impacts of irradiation type on circulating lymphocytes. Tuning the physiology-based parameters could be a potential approach to building a predictive model in humans. Parameters might need to be re-estimated to fit with effects in humans. Further research and analysis on interactions between leucocyte subpopulations is an area of investigation and may have implications for the choice of radiotherapy modalities and their combination with immunotherapy in brain cancer treatment.

## Acknowledgement

We would like to thank Alison Johnson for her time reading and editing the language of this manuscript.

## Disclosure statement

The authors report there are no competing interests to declare

## Biographical note

Thao-Nguyen Pham, MSc, Pharm is a pharmacist and PhD student in cancer biology and biomathematics. Julie Coupey, MSc is a PhD student in cancer biology. Jérôme Toutain, MSc is a specialist in radiation experiment in animals. Serge M. Candéias, PhD is a specialist in immunology. Gaël Simonin, MSc is a PhD in physics and engages in Monte Carlo simulation. Marc Rousseau, PhD is a specialist in radiotherapy and proton therapy. Omar Touzani, PhD is a professor in physiology and cancer biology. Juliette Thariat, MD, PhD is an oncologist and professor in radiotherapy. Samuel Valable, PhD is a specialist in biophysics and radiotherapy

## Funding

This project has received financial support from the CNRS through the 80|Prime program, Ligue Contre le Cancer, and French National Agency for Research 'Investissements d'Avenir' (n°ANR-10-EQPX1401). SC work is funded in part by the LABEX PRIMES (grant number ANR-11-LABX-0063).

## ORCID

Serge M. Candéias  <http://orcid.org/0000-0003-2257-5529>  
 Juliette Thariat  <http://orcid.org/0000-0003-4755-496X>  
 Samuel Valable  <http://orcid.org/0000-0003-0355-0270>

## Data availability statement

All other data will be made available upon reasonable request made to the corresponding author.

## References

- Ahmed MM, Hodge JW, Guha C, Bernhard EJ, Vikram B, Coleman CN. 2013. Harnessing the potential of radiation-induced immune modulation for cancer therapy. *Cancer Immunol Res.* 1(5):280–284. doi:10.1158/2326-6066.CIR-13-0141
- Bilen MA, Martini DJ, Liu Y, Lewis C, Collins HH, Shabto JM, Akce M, Kissick HT, Carthon BC, Shaib WL, et al. 2019. The prognostic and predictive impact of inflammatory biomarkers in patients who have advanced-stage cancer treated with immunotherapy: Inflammatory Biomarkers in Immunotherapy. *Cancer.* 125(1):127–134. doi:10.1002/cncr.31778
- Blum KS, Pabst R. 2007. Lymphocyte numbers and subsets in the human blood. *Immunol Lett.* 108(1):45–51. doi:10.1016/j.imlet.2006.10.009
- Buescher ES, Gallin JI. 1984. Radiation effects on cultured human monocytes and on monocyte-derived macrophages. *Blood.* 63(6):1402–1407. doi:10.1182/blood.V63.6.1402.1402
- Chen F, Jin J-Y, Hui TSK, Jing H, Zhang H, Nong Y, Han Y, Wang W, Ma L, Yi F, et al. 2022. Radiation induced lymphopenia is associated



- with the effective dose to the circulating immune cells in breast cancer. *Front Oncol.* 12:768956. doi:10.3389/fonc.2022.768956
- Cho Y, Kim J, Yoon H, Lee C, Keum K, Lee I. 2018. The prognostic significance of neutrophil-to-lymphocyte ratio in head and neck cancer patients treated with radiotherapy. *J Clin Med.* 7(12):512. doi:10.3390/jcm7120512
- Coupey J, Pham TN, Toutain J, Ivanova V, Hue E, Helaine C, Ismail A, Saulnier R, Simonin G, Rousseau M, et al. 2024. Investigating the effects of protons versus x-rays on radiation-induced lymphopenia after brain irradiation. *bioRxiv.* <https://doi.org/10.1101/2024.03.02.583088>
- de Andrade Carvalho H, Villar RC. 2018. Radiotherapy and immune response: the systemic effects of a local treatment. *Clinics (Sao Paulo).* 73(suppl 1):e557s. doi:10.6061/clinics/2018/e557s
- Ellsworth SG. 2018. Field size effects on the risk and severity of treatment-induced lymphopenia in patients undergoing radiation therapy for solid tumors. *Adv Radiat Oncol.* 3(4):512–519. doi:10.1016/j.adro.2018.08.014
- Ellsworth SG, Yalamanchali A, Lautenschlaeger T, Grossman SA, Grassberger C, Lin SH, Mohan R. 2022. Lymphocyte depletion rate as a biomarker of radiation dose to circulating lymphocytes during fractionated partial-body radiation therapy. *Adv Radiat Oncol.* 7(5):100959. doi:10.1016/j.adro.2022.100959
- Fadul CE, Fisher JL, Gui J, Hampton TH, Côté AL, Ernstoff MS. 2011. Immune modulation effects of concomitant temozolomide and radiation therapy on peripheral blood mononuclear cells in patients with glioblastoma multiforme. *Neuro Oncol.* 13(4):393–400. doi:10.1093/neuonc/noq204
- Farese AM, Hankey KG, Cohen MV, MacVittie TJ. 2015. Lymphoid and myeloid recovery in rhesus macaques following total body X-irradiation. *Nat Rev Phys.* 109(5):414–426. doi:10.1097/hp.0000000000000348
- Gaikwad U, Bajpai J, Jalali R. 2023. Combinatorial approach of immuno-proton therapy in cancer: rationale and potential impact. *Asia Pac J Clin Oncol. Early View.* doi:10.1111/ajco.13966
- Galluzzi L, Aryankalayil MJ, Coleman CN, Formenti SC. 2023. Emerging evidence for adapting radiotherapy to immunotherapy. *Nat Rev Clin Oncol.* 20(8):543–557. doi:10.1038/s41571-023-00782-x
- Ghanavati S. 2017. Quantitative Analysis and Comparison of Cerebrovasculature in Common Mouse Strains: C57BL/6, CD-1, CBA, and 129/Sv using Imaging, Automatic Segmentation and Labelling of the Cerebral Vessels. Graduate Department of Medical Biophysics, University of Toronto.
- Hall C, Lueshen E, Mošat' A, Linninger AA. 2012. Interspecies scaling in pharmacokinetics: a novel whole-body physiologically based modeling framework to discover drug biodistribution mechanisms in vivo. *J Pharm Sci.* 101(3):1221–1241. doi:10.1002/jps.22811
- Hammi A, Paganetti H, Grassberger C. 2020. 4D blood flow model for dose calculation to circulating blood and lymphocytes. *Phys Med Biol.* 65(5):055008. doi:10.1088/1361-6560/ab6c41
- He H, Geng T, Chen P, Wang M, Hu J, Kang L, Song W, Tang H. 2016. NK cells promote neutrophil recruitment in the brain during sepsis-induced neuroinflammation. *Sci Rep.* 6(1):27711. doi:10.1038/srep27711
- Holley TR, Van Epps DE, Harvey RL, Anderson RE, Williams RC. 1974. Effect of high doses of radiation on human neutrophil chemotaxis, phagocytosis and morphology. *Am J Pathol.* 75(1):61–72.
- Hollowell JG, Littlefield LG. 1968. Chromosome damage induced by plasma of X-rayed patients: an indirect effect of X-ray. *Proc Soc Exp Biol Med.* 129(1):240–244. doi:10.3181/00379727-129-33295
- Holub K, Vargas A, Biete A. 2020. Radiation-induced lymphopenia: the main aspects to consider in immunotherapy trials for endometrial and cervical cancer patients. *Clin Transl Oncol.* 22(11):2040–2048. doi:10.1007/s12094-020-02345-3
- Huang J, DeWees TA, Badiyan SN, Speirs CK, Mullen DF, Fergus S, Tran DD, Linette G, Campian JL, Chicoine MR, et al. 2015. Clinical and dosimetric predictors of acute severe lymphopenia during radiation therapy and concurrent temozolomide for high-grade glioma. *Int J Radiat Oncol Biol Phys.* 92(5):1000–1007. doi:10.1016/j.ijrobp.2015.04.005
- Jin J-Y, Gu A, Wang W, Oleinick NL, Machtay M, (Spring) Kong F-M. 2020. Ultra-high dose rate effect on circulating immune cells: A potential mechanism for FLASH effect? *Radiother Oncol.* 149:55–62. doi:10.1016/j.radonc.2020.04.054
- Kapoor V, Khudanyan A, de la Puente P, Campian J, Hallahan DE, Azab AK, Thotala D. 2015. Stem cell transfusion restores immune function in radiation-induced lymphopenic C57BL/6 mice. *Cancer Res.* 75(17):3442–3445. doi:10.1158/0008-5472.CAN-15-1412
- Ladbury CJ, Rusthoven CG, Camidge DR, Kavanagh BD, Nath SK. 2019. Impact of radiation dose to the host immune system on tumor control and survival for stage III non-small cell lung cancer treated with definitive radiation therapy. *Int J Radiat Oncol Biol Phys.* 105(2):346–355. doi:10.1016/j.ijrobp.2019.05.064
- Leblond MM, Pères EA, Helaine C, Gérault AN, Moulin D, Anfray C, Divoux D, Petit E, Bernaudin M, Valable S. 2017. M2 macrophages are more resistant than M1 macrophages following radiation therapy in the context of glioblastoma. *Oncotarget.* 8(42):72597–72612. doi:10.18632/oncotarget.19994
- Lesueur P, Calugaru V, Nauraye C, Stefan D, Cao K, Emery E, Reznik Y, Habrand JL, Tessonier T, Chaikh A, et al. 2019. Proton therapy for treatment of intracranial benign tumors in adults: A systematic review. *Cancer Treat Rev.* 72:56–64. doi:10.1016/j.ctrv.2018.11.004
- Macintyre AN, French MJ, Sanders BR, Riebe KJ, Shterev ID, Wiehe K, Hora B, Evangelous T, Dugan G, Bourland JD, et al. 2021. Long-term recovery of the adaptive immune system in rhesus macaques after total body irradiation. *Adv Radiat Oncol.* 6(5):100677. doi:10.1016/j.adro.2021.100677
- Ménétrier-Caux C, Ray-Coquard I, Blay J-Y, Caux C. 2019. Lymphopenia in cancer patients and its effects on response to immunotherapy: an opportunity for combination with cytokines? *J Immunotherapy Cancer.* 7(1):85. doi:10.1186/s40425-019-0549-5
- Miszczyk J, Rawojć K, Panek A, Borkowska A, Prasanna PGS, Ahmed MM, Swakoń J, Galaś A. 2018. Do protons and X-rays induce cell-killing in human peripheral blood lymphocytes by different mechanisms? *Clin Transl Radiat Oncol.* 9:23–29. doi:10.1016/j.ctro.2018.01.004
- Mohan R, Liu AY, Brown PD, Mahajan A, Dinh J, Chung C, McAvoys S, McAleer MF, Lin SH, Li J, et al. 2021. Proton therapy reduces the likelihood of high-grade radiation-induced lymphopenia in glioblastoma patients: phase II randomized study of protons vs photons. *Neuro Oncol.* 23(2):284–294. doi:10.1093/neuonc/noaa182
- Murshed H. 2019. Proton radiation therapy. In *Fundamentals of radiation oncology.* Elsevier; [accessed 2022 Dec 6]. p. 161–171. doi:10.1016/B978-0-12-814128-1.00009-X
- Nakamura N, Kusunoki Y, Akiyama M. 1990. Radiosensitivity of CD4 or CD8 positive human T-lymphocytes by an in vitro colony formation assay. *Radiat Res.* 123(2):224–227.
- Orth M, Lauber K, Niyazi M, Friedl AA, Li M, Maihöfer C, Schüttrumpf L, Ernst A, Niemöller OM, Belka C. 2014. Current concepts in clinical radiation oncology. *Radiat Environ Biophys.* 53(1):1–29. doi:10.1007/s00411-013-0497-2
- Park H-R, Jung U. 2021. Depletion of NK cells resistant to ionizing radiation increases mutations in mice after whole-body irradiation. *In Vivo.* 35(3):1507–1513. doi:10.21873/invivo.12403
- Pham T-N, Coupey J, Candeias SM, Ivanova V, Valable S, Thariat J. 2023. Beyond lymphopenia, unraveling radiation-induced leucocyte subpopulation kinetics and mechanisms through modeling approaches. *J Exp Clin Cancer Res.* 42(1):50. doi:10.1186/s13046-023-02621-4
- R Core Team. 2021. R: A Language and Environment for Statistical Computing [Internet]. <https://www.R-project.org/>.
- Shohan J. 1916. Some theoretical considerations on the present status of roentgen therapy. *Boston Med Surg J.* 175(10):321–327. doi:10.1056/NEJM191609071751001
- Tang C, Liao Z, Gomez D, Levy L, Zhuang Y, Gebremichael RA, Hong DS, Komaki R, Welsh JW. 2014. Lymphopenia association with gross tumor volume and lung v5 and its effects on non-small cell lung cancer patient outcomes. *Int J Radiat Oncol Biol Phys.* 89(5):1084–1091. doi:10.1016/j.ijrobp.2014.04.025
- Thariat J, Hannoun-Levi J-M, Sun Myint A, Vuong T, Gérard J-P. 2013. Past, present, and future of radiotherapy for the benefit of patients. *Nat Rev Clin Oncol.* 10(1):52–60. doi:10.1038/nrclinonc.2012.203
- Therneau T, Atkinson B, Ripley B. 2022. rpart: Recursive partitioning and regression trees. <https://CRAN.R-project.org/package=rpart>
- Venkatesulu BP, Sharma A, Pollard-Larkin JM, Sadagopan R, Symons J, Neri S, Singh PK, Tailor R, Lin SH, Krishnan S. 2019. Ultra



- high dose rate (35Gy/sec) radiation does not spare the normal tissue in cardiac and splenic models of lymphopenia and gastrointestinal syndrome. *Sci Rep.* 10(1):11018. doi:[10.1038/s41598-019-53562-y](https://doi.org/10.1038/s41598-019-53562-y)
- Widick P, Winer ES. 2016. Leukocytosis and leukemia. *Prim Care.* 43(4):575–587. doi:[10.1016/j.pop.2016.07.007](https://doi.org/10.1016/j.pop.2016.07.007)
- Wu Q, Allouch A, Martins I, Brenner C, Modjtahedi N, Deutsch E, Perfettini J-L. 2017. Modulating both tumor cell death and innate immunity is essential for improving radiation therapy effectiveness. *Front Immunol.* 8:613. doi:[10.3389/fimmu.2017.00613](https://doi.org/10.3389/fimmu.2017.00613)
- Yovino S, Kleinberg L, Grossman SA, Narayanan M, Ford E. 2013. The etiology of treatment-related lymphopenia in patients with malignant gliomas: modeling radiation dose to circulating lymphocytes explains clinical observations and suggests methods of modifying the impact of radiation on immune cells. *Cancer Invest.* 31(2):140–144. doi:[10.3109/07357907.2012.762780](https://doi.org/10.3109/07357907.2012.762780)
- Zhang Z, Liu X, Chen D, Yu J. 2022. Radiotherapy combined with immunotherapy: the dawn of cancer treatment. *Sig Transduct Target Ther.* 7(1):258. doi:[10.1038/s41392-022-01102-y](https://doi.org/10.1038/s41392-022-01102-y)